Hybrid Gridded Tomography

By

Ian F. Jones
Mick Sugrue
Pierre Hardy

GX Technology, 180 High Street, Egham, Surrey TW20 9DN, UK

First Break
V 25
April 2007
P15-21

Corresponding Author
Ian F. Jones
ijones@gxt.com

Hybrid Gridded Tomography: Jones et al

Hybrid Gridded Tomography
Ian F. Jones, Mick J. Sugrue, Pierre B. Hardy
GX Technology, UK

Introduction

Historically, the practice in velocity model building usually resorted to one of two approaches: the layer-based and the gridded (Jones, 2003). Additionally, in recent years both approaches have relied on dense continuous autopicking of residual velocity error to provide the subsequent inversion process with more reliable input data (Jones, et al, 2000).

For North Sea type environments where sedimentary interfaces delimit changes in the velocity field and the geology 'lends itself' to a layer-based model representation, a layer-based approach to velocity model building has hitherto been commonly used. In other words, we have encouraged preconceived bias, as we consider it to be a meaningful geological constraint on the solution.

Conversely, the gridded approach to velocity model building is usually adopted in environments where the velocity regime is decoupled from the sedimentation, and is governed primarily by vertical compaction gradients (velocity increasing with depth), controlled by de-watering, with iso-velocity contours sub-paralleling the sea bed.

However, a purely gridded tomographic approach (Hardy, 2003, Sugrue et al, 2004) is sometimes unable to preserve rapid vertical variations in velocity, and moreover, for seismically transparent layers with large velocity contrasts, we still need to constrain the model with interpretational input (Campbell, et al, 2005; Evans et al, 2005). With this in mind, we have here adopted a modification to the purely gridded approach to incorporate layer constraints at major vertical velocity boundaries

In the examples considered here, which are typical of many North Sea fields, we have a thick chalk sequence, with a vertical compaction gradient within the chalk. The nature of these compaction gradients can be quite complex, with many subdivisions that are not obviously manifest in terms of a clear and laterally continuous seismic response. Due to compaction within the chalk, we can move from a near constant velocity regime in the uppermost part of the chalk, to a steep compaction gradient regime, and then back to a constant (high) velocity region at the base of the chalk, where the chalk has been compressed as much as it can be by the overburden pressure.

Two classes of error can occur in building a model for such chalk bodies:

a). The internal layering in the chalk may not be sufficiently well represented in the layered model, due to the difficulty in picking a clear event when we have a change in compaction gradient rather than a sharp change in reflectivity

b). Errors in the estimate of the values for the compaction gradient can manifest themselves as apparent anisotropy (Alkhalifa, 1997; Jones, et al, 2003)

Both of these errors will result in sub-optimal imaging, including the lateral mispositioning of faults (Alkhalifa & Tsvankin, 1995; Hawkins, et al, 2001).

Styles of Layer Constraint for Hybrid Tomography

Within the tomographic framework, we define two styles of constraint layer: the 'hard' and the 'soft'.

A hard constraint layer (such as at the sea bed, top and base chalk, or pickable near-surface channel), would result in the model being left unchanged in subsequent iterations ABOVE the picked layer. As such we move from a global tomography to a non-global layer stripping tomography (but still use a gridded tomography with the layered constraint: i.e. the hybrid tomography).

A soft constraint layer would be used if the layer being picked was very uncertain, as is often the case for an ill-defined near-surface channel or the seismically transparent top-salt picks in the Zechstein sequence of the North Sea. In this latter case, we profit from having the salt velocity inserted in the model below the tentatively picked layer, which helps the convergence of the inversion, even though we allow the tomography to change both the velocity in the picked layer and the layer position itself. In this case the model above the soft-constraint pick can change.

Velocity Model Building & Pre-Stack Depth Migration

In the following examples, all taken from the North Sea, we followed a similar route. The initial depth velocity model was built from stacking velocities converted to interval velocity in depth. The water bottom was picked and gridded as a hard constraint, based on an initial migration to create the water layer in the depth interval velocity model. Following this step, we proceeded to several iterations of hybrid gridded tomographic update (Hardy, 2003), as follows (figure 1):

a) run 3D preSDM on a specified grid, outputting full offset gathers continuously along velocity lines
b) run a plane-wave autopicker on all gathers, to determine dip, coherency, and residual curvature fields
c) input autopicked picked data into tomography and update velocity field

For the strong vertical velocity contrasts (and when anisotropy is to be incorporated), horizons are picked as a constraint on the gridded tomography (the hybrid approach).

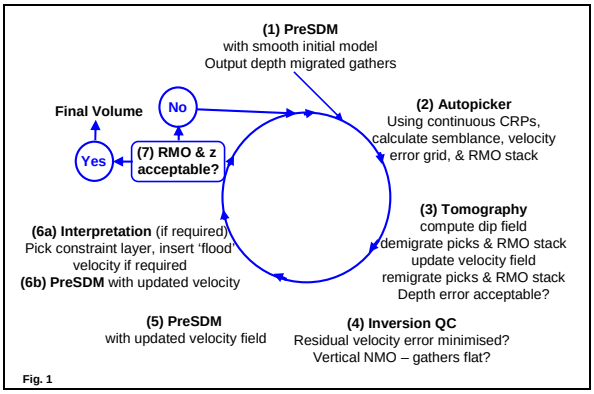

Figure 1: schematic of iterative hybrid update procedure, commencing with CRP gathers from preSDM with a smooth initial model.

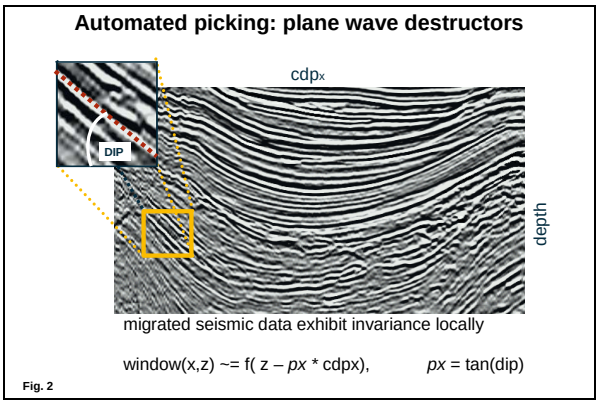

Figure 2: In a small window, a seismic event looks like a linear dipping segment. We solve for the dip of this segment, and on the gather, we solve for a fit to the residual moveout, either piecewise for each offset, or as a general fit across all offsets

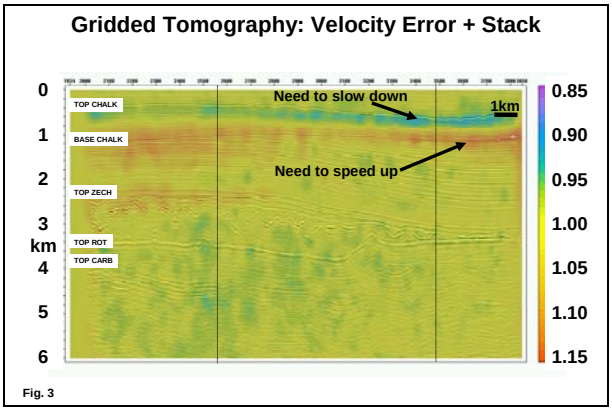

Figure 3: residual curvature on the CRP gathers: A value of 1.0 indicates flat CRP gathers, <1.0 indicates current velocity too fast, >1.0 indicates current velocity too slow.

Constraint layers were picked where we anticipated significant vertical velocity contrasts. In these iterations, an additional step was performed:

d). using the updated velocity from the previous tomographic update (c), run a new 3D preSDM outputting a restricted offset stack for the structural interpretation (on a 50m * 50m grid).

Anisotropy is readily incorporated into this workflow as we have picked horizons with which to calibrate against available well control. In addition, using a picked layer as a 'hard' constraint will preserve anisotropic depth calibration during subsequent tomographic iterations.

The auto-picking algorithm is based on the plane-wave destructor principle (Claerbout, 1992; Hardy, 2003). A user-defined 3D probe containing trace portions for different CDP's and offsets is moved about the data. At each position, the slope along the CDP axis and residual curvature across the offset axis is computed (via least squares minimization) (figure 2). The quality of these estimates is also computed. As a result of this picking, a 3D slope field and residual move-out estimate are determined (figure 3). For inverting large 3D problems, a conjugate gradient approach is used. As a by-product of the autopicking, we also obtained a residual moveout (RMO) corrected stack of the image (figure 4). This is a good indication of whether the autopicker has found the correct residual moveout in preparation for the tomographic update, and can indicate if residual multiple energy is being inadvertently picked.

Following the autopicking, the tomography (van Trier, 1990, Jeannot & Hardy, 1994, Hardy & Jeannot, 1999) takes the RMO and dip field measurements in conjunction with weights based on the 'quality' of the autopicks, and generates a tomographic solution to minimize the residual move-out values.

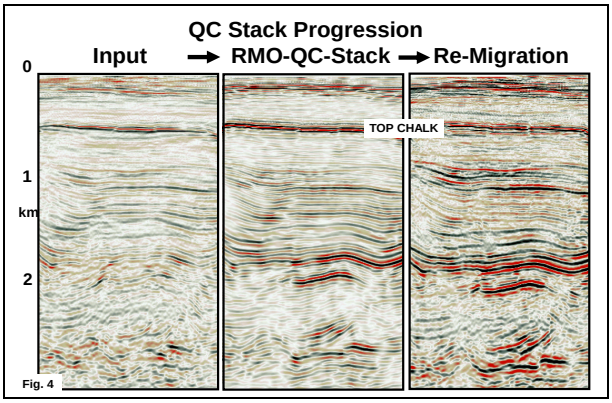

Figure 4: left: stack of CRP gathers from the current iteration. Centre: after the autopicking, an RMO correction is applied to these gathers using the picked residual curvature, thus improving the stack, but not producing movement in the events. Right: new image from re-migration after tomographic update of the velocity, based on the picked RMO residuals

Following completion of the model building, an amplitude preserving 3D Kirchhoff pre-stack depth migration is usually performed outputting all gathers on the dense final output grid. For more demanding geological environments, the tomography is supplemented by picking horizons on wavefield extrapolation (WE) migrated images, and/or running the autopicker on WE migrated angle gathers.

Example 1: Gas Play, Southern North Sea.
The first example is taken from a case study from a four survey merge covering some 430sq.km which was reprocessed to yield a coherent single input volume for 3D preSDM imaging (Campbell, et al, 2005).

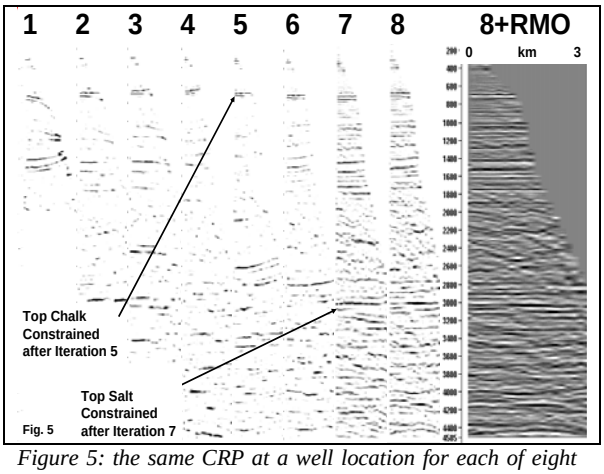

Figure 5: the same CRP at a well location for each of eight iterations of model update. Right: the last iteration after RMO for final stack. The top chalk pick was a 'hard' constraint, so nothing changes above it after iteration 5. However, the top salt pick was used as a 'soft' constraint, so the tomography was free to modify the model above the salt.

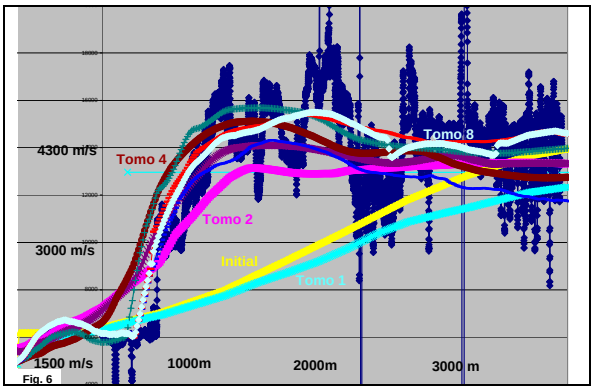

Figure 6: The well sonic for the gathers shown in fig.5, and the corresponding migration velocity profile for successive iterations of model update. The well is not used explicitly in the tomography, but used as a QC and/or for anisotropy parameter estimation.

Successive iterations of the tomography (figure 5) converged to a smooth representation of the sonic well log, even though this is not an explicit constraint of the update procedure (figure 6). Good well-ties were obtained during the model building, and isotropic migration was employed (figure 7). The top chalk event is a clear marker throughout the survey, and represents a rapid vertical increase in velocity; hence it was incorporated as a 'hard layer constraint at iteration five of the model building. Conversely, the top Zechstein evaporite event has a strong velocity contrast with the surrounding sediments, but a variable impedance contrast, so can become seismically transparent at times, making it difficult to pick in the section. We inserted the (approximate) top Zechstein horizon as a 'soft' constraint in the tomography: thus we profited from having the high salt velocity in the model for the subsequent iteration, but permitted the tomography to modify the velocity (and hence the position of the event) so as to avoid biasing the model.

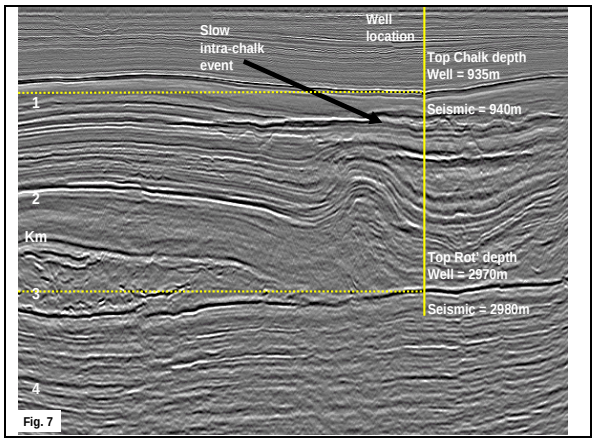

Figure 7: final image at the well location.

Example 2: Carboniferous Gas Play, Southern North Sea.
The second example involves an eight survey merge covering some 1500 sq.km which was reprocessed to yield a coherent single input volume for both preSTM and preSDM isotropic imaging for exploration evaluation (Papouin, et al, 2004, Evans, et al, 2005). After an initial model building and migration project was completed using purely gridded tomography, we revisited a portion of the data over a new development well, using the hybrid gridded technique. The resulting images show good resolution of the Zechstein and Carboniferous section (Spencer at al, 2004), improved on vintage processing.

The first constraint layer picked was the top chalk (figure 8). Here we see a portion of a 'crater' variously described in the literature as a meteorite impact crater and also a salt withdrawal structure. We note concentric rims around this feature, which in vertical profile show-up as ripples on the top chalk (figures 9 & 10). In the gridded model result, we can clearly see an imprint of the top chalk structure on the

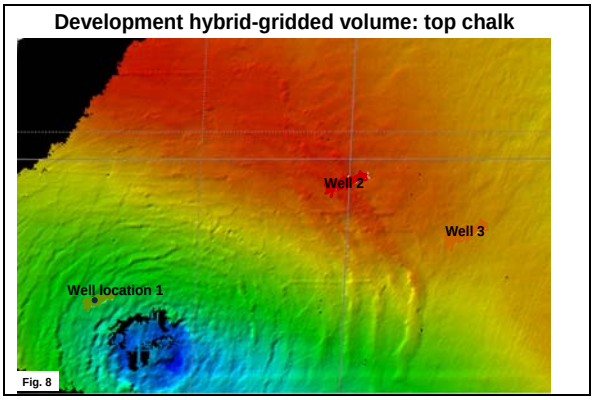

Figure 8: Top Chalk horizon, picked as the first 'hard' layer constraint for the hybrid tomography. Concentric rings associated with the crater-like structure are visible in the lower left.

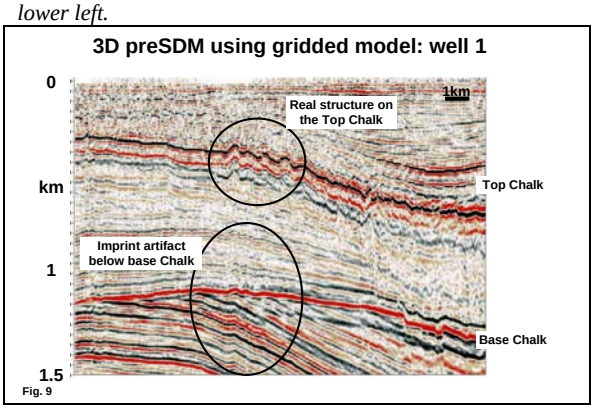

Figure 9: Inline depth section, intersecting well location 1 from the purely gridded tomographic mode1. The corrugations on the top chalk, associated with the crater-like feature are clearly visible. Below these corrugations, we see an imaging artifact resulting from velocity smearing through the top chalk.

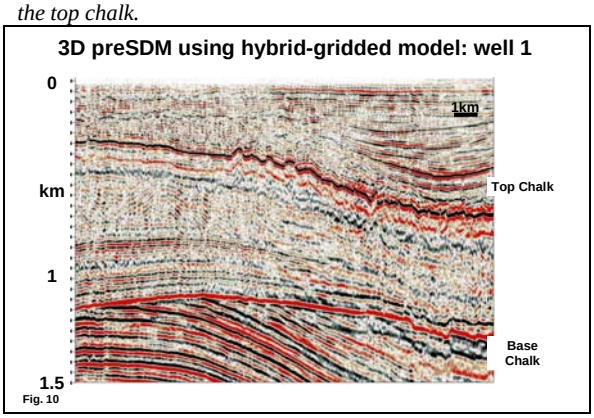

Figure 10: Inline depth section, intersecting well location 1 from the hybrid gridded model. The corrugations on the top chalk, associated with the crater-like feature are still clearly visible. However the imprint of these corrugations below the top chalk has been removed, producing a more reasonable image.

base chalk, and other events. Using the hybrid approach, where the top chalk is inserted in the model as a hard constraint, with a gridded velocity field both above and below, the imprint has been removed, and the sub-chalk image improved.

Just above the target level, in figures 11 & 12, we see the base Permian unconformity and the top Rotliegend event. In figure 11, showing the image from the hybrid approach, we see a pick of the Rotliegend shown in yellow. This pick is superimposed on the older (purely) gridded result in figure 12. Compared to the hybrid pick, the old version of the Rotliegend shows a long wavelength structural flexure, which is probably incorrect. The new image shows better focusing on the steeply dipping Carboniferous events sub-cropping the base Permian unconformity, as well as having more consistent well ties.

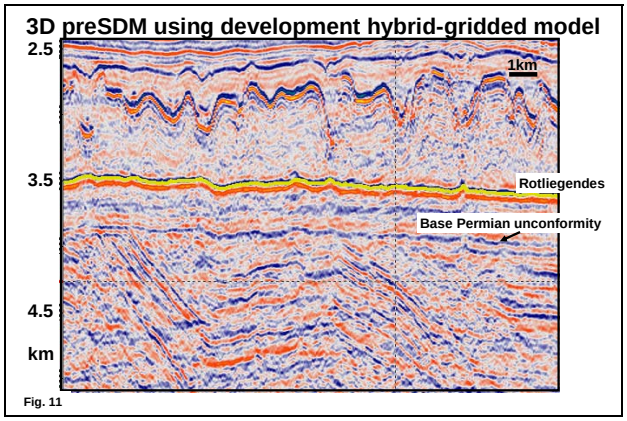

Figure 11: Hybrid gridded image showing the Rotliegend and base Permian unconformity. The Rotliegend pick is shown in yellow,

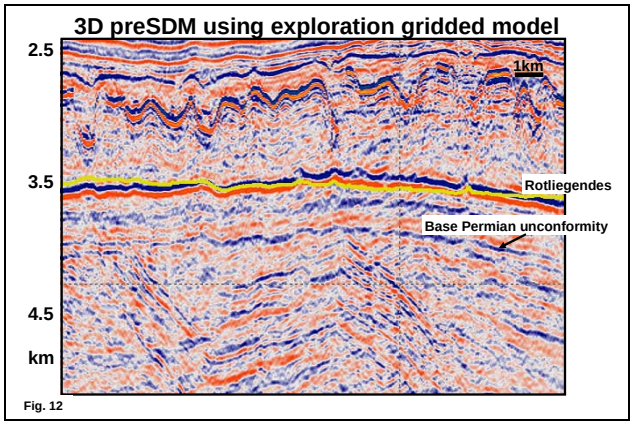

Figure 12: Purely gridded image showing the Rotliegend and base Permian unconformity: the Rotliegend pick from figure 11 is superimposed in yellow, showing a long-wavelength difference between the images at target level, which is most likely a consequence of velocity error in the overburden in the older processing.

Example 3: South Arne, Danish North Sea.
The data shown here come from the Hess South Arne field in the Danish sector of the Southern Central Graben of the North Sea (Sugrue et al, 2004). The maximum offset was 4200m, providing sufficient velocity resolution at target depth (~3000m) with a reasonable frequency spectrum (~60Hz). We can see an area with a benign flat lying overburden, below which compressional deformation and structural inversion throughout the Cretaceous has resulted in a structural high at the level of the Chalk reservoir sequence. The chalk sequence thins over this elongate anticlinal ridge and asymmetrically thickens off-structure with a thicker chalk sequence developed to the right (West) of the ridge. Above the structure, gas leakage gives rise to brightening of the seismic image (figure 13).

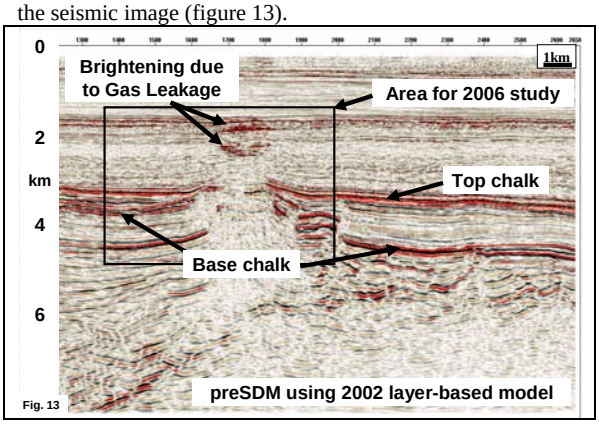

Figure 13: Crestal line from the South Arne field showing the chalk ridge

To assist in the interpretation of a recent (2006) well placement, a detailed anisotropic hybrid gridded tomographic project was conducted in 2006, with picked horizon constraint layers. Previously, in 2002, an exploration project was conducted on these data, and following that in 2004 a development project was undertaken.

Consequently we have a unique opportunity to compare three different model building approaches (layered, gridded, and hybrid) that have the same underlying tomography and migration algorithm (as well as the same input data).

The model building and migration for the exploration project was performed isotropically in 2002 using iterative CRP scanning with a layered model incorporating the top and base chalk as the main velocity contrasts, with a single compaction gradient within the chalk. Both the thin and the thick chalk sequences were represented by a single layer, as the intermediate intra-chalk horizons were discontinuous. With hindsight, it would have been better to include a layer within the thick chalk sequence to account for the changes in the compaction gradient regime.

Whereas the exploration 3D preSDM project processed in 2002 was isotropic, the more detailed production 3D preSDM (which employed purely gridded tomography) processed in 2004, was anisotropic (Thomsen, 1986). To facilitate a fairer comparison, we re-ran the gridded model building isotropically on a 2D crestal line over the reservoir structure to exemplify the procedures involved in the purely gridded tomography.

For the most-part the velocity remains unchanged down to the top chalk, other than for the introduction of a low velocity zone which corresponds to the gas bright spots. Within, and just below the chalk however, we see dramatic changes in the velocity introduced by the gridded approach. To the right of the crestal ridge, the simple compaction gradient of the layered model is replaced by a more complex regime, and to the left of the ridge, we see the introduction of a low velocity layer below the chalk, feeding up into the crestal structure.

We observe that the upper part of the chalk is better described by a near-constant velocity region, and that the strong gradient regime commences deeper within the chalk. Importantly, the vertical compaction gradient is not constant laterally across the chalk body: when building a layered model, it is usual to keep a constant gradient in a given layer, as we seldom have sufficient well control to justify lateral variation in layered models.

The structure below the chalk is much better defined using the gridded model. Doubtless, a comparable result could be achieved using a layered model, if much more time and effort was put into the layered model building.

In figure 14, we contrast results from the three model building approaches, showing the velocity model and corresponding 3D preSDM images. The comparisons are not quite fair, as the 2002 exploration layer based result was obtained using isotropic migration, and the anisotropy parameters for the 2004 gridded and 2006 hybrid gridded preSDMs are slightly different. However, the broad conclusions still hold: we see a general improvement in image quality (the pre-processing being the same for all migrations), better well-ties, and good lateral positioning control vis a vis well penetrations of faults.

Discussion
We have briefly introduced strategies for building models for complex geology, and contrasted results for update in a layered model building scheme, a dense auto-picking-driven gridded tomographic approach, and a hybrid-gridded approach. Although it should be possible to achieve a detailed model building procedure using a layered approach, it has proven to be more practical to use the gridded strategy when we have subtle lateral variations in the velocity structure, combining the velocity grids with layer constraints when we have large vertical velocity contrasts.

Acknowledgements
The authors wish to thank our various UK clients for kind permission to show the data in the first two examples, and to Hess Denmark, and partners for kind permission to show their data, and also to our colleagues for help with this work. The authors wish to thank the management of GX Technology and its parent company, Input/Output, for permission to publish the results of this study.

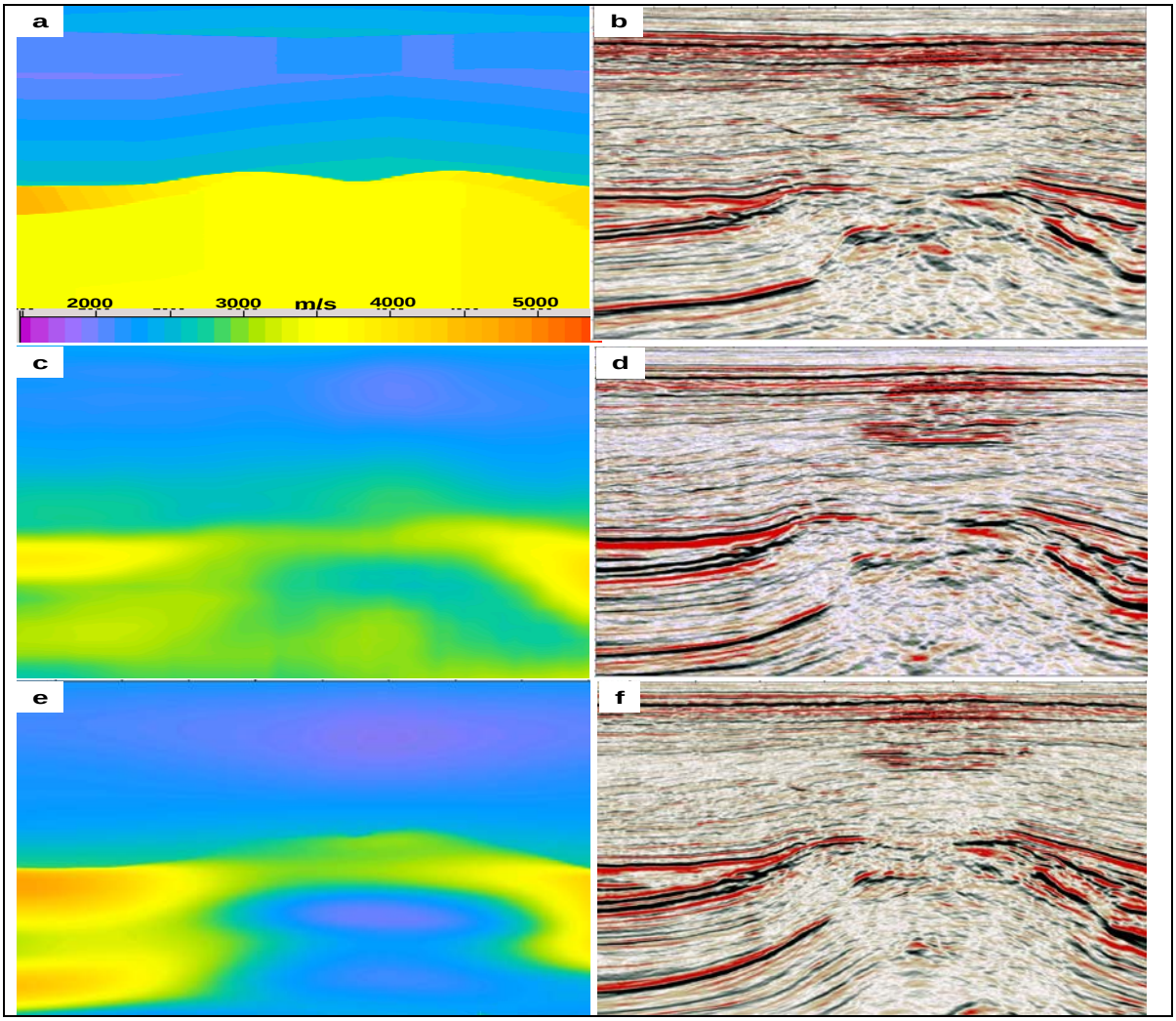

Figure 14: model and image for the three model building approaches, showing a successive improvement

References

Alkhalifah, T., 1997, Velocity analysis using nonhyperbolic moveout in transversely isotropic media; Geophysics, 62, 1839-1854.

Alkhalifah, T., & Tsvankin, I., 1995, Velocity analysis for transversely isotropic media; Geophysics, 60, 1550-1566.

Campbell, A.G., Evans, E., Judd, D, Jones, I.F., Elam, S., 2005, A Southern North Sea Multi-Survey preSDM: 67th annual meeting of the European Association of Exploration Geophysicists. B025.

Claerbout, J.F., 1992, Earth Soundings Analysis: PVI, Blackwell Scientific Publications.

Evans, E., Papouin, M., Abedi, S., Gauer, M, Smith, P., Jones, I.F., 2005, Southern North Sea preSDM imaging using hybrid gridded tomography: 75th annual meeting of the Society of Exploration Geophysicists. 2530-2533.

Hardy, P. and Jeannot, J. -P., 1999, 3-D reflection tomography in time-migrated space: 69th annual meeting of the Society of Exploration Geophysicists, 1287-1290.

Hardy, P.B., 2003, High resolution tomographic MVA with automation, SEG/EAGE summer research workshop, Trieste.

Hawkins, K., Leggot, R., Williams, G., & Kat, H., 2001, Addressing anisotropy in 3D pre-stack depth migration: a case study from the Southern North Sea. The Leading Edge, 20, 528-543.

Jeannot, J. P. and Hardy, P., 1994, Practical traveltime tomography of 2-D reflection seismic data: 56th Mtg.: annual meeting of the European Association of Exploration Geophysicists. P060.

Jones, I.F., Baud, H., Ibbotson,K., Audebert, F., 2000, Continuous 3D preSDM velocity analysis: The Leading Edge, 19, 263-269.

Jones, I.F., 2003, A review of 3D preSDM velocity model building techniques. First Break, 21, 45-58.

Jones, I.F., Bridson, M.L., & Bernitsas, N, 2003, Anisotropic Ambiguities in TI Media. First Break, 21, 31-37.

Papouin, M., Gauer, M., Abedi, S., Evans, E., Smith, P., Jones, I.F., 2004: Improving Seismic Data Quality in the Southern North Sea, Carboniferous, proceedings of PESGB PETEX biennial meeting.

Spencer, A., Cooper, D., 2004, Keys to successful exploration of the SNS Carboniferous, proceedings of PESGB PETEX biennial meeting.

Sugrue, M., Jones, I.F., Evans, E., Fairhead, S., Marsden, G., 2004, Velocity estimation in complex chalk,. Geophysical Prospecting, 52, 683-691.

van Trier, J., 1990, Reflection tomography after depth migration: Field data results: 60th annual meeting of the Society of Exploration Geophysicists, 1279-1282.